Anat. Histol. Embryol. **34,** 52–55 (2005)

ISSN 0340–2096

Department of Morphology (Anatomy and Embryology), Veterinary Faculty, University of Las Palmas de Gran Canaria, Spain

Anatomy of the Cranioencephalic Structures of the Camel (*Camelus dromedarius* L.) by Imaging Techniques: A Magnetic Resonance Imaging Study

A. Arencibia[1]*, M. A. Rivero[1], F. Gil[2], J. A. Ramírez[1], J. A. Corbera[3], G. Ramírez[2] and J. M. Vázquez[2]

Addresses of authors: [1]Department of Morphology, University of Las Palmas de Gran Canaria, Las Palmas de Gran Canaria 35416, Spain; [2]Department of Anatomy, University of Murcia, Murcia 30100, Spain, [3]Department of Animal Medicine and Surgery, University of Las Palmas de Gran Canaria, Las Palmas de Gran Canaria 35416, Spain; *Corresponding author: e-mail: aarencibia@dmor.ulpgc.es

With 5 figures

Received November 2003; accepted for publication April 2004

Summary

The objective of this study was to define the anatomy of the cranioencephalic structures and associated formations in camel using magnetic resonance imaging (MRI). MR images were acquired in sagittal, transverse and oblique dorsal planes, using spin-echo techniques, a magnet of 1.5 T and a standard human body coil. MR images were compared with corresponding frozen cross-sections of the head. Different anatomic structures were identified and labelled at each level. The resulting images provided excellent soft tissue contrast and anatomic detail of the brain and associated structures of the camel head. Annotated MR images from this study are intended to be a reference for clinical imaging studies of the head of the dromedary camel.

Introduction

Magnetic resonance imaging (MRI) is a diagnostic technique that has advanced significantly and it is now routinely used in human medicine for the study and evaluation of anatomy (Goncalves-Ferreira et al., 2001) and pathology (Arnold and Matthews, 2002) in many structures of the central nervous system. In small animals, is frequently used to evaluate the head (Kraft et al., 1989; Karkkainen et al., 1991; Morgan et al., 1994; Hudson et al., 1995). The use of MRI in large animal medicine is currently limited by the logistical problems of acquiring MR images. Some MRI studies on horses' head exist (Morgan et al., 1993; Chaffin et al., 1997; Arencibia et al., 2000). An accurate interpretation of the planimetric MR normal anatomy is necessary for the study and evaluation of pathologic tissues.

The objective of this study is to provide an overview of the normal cross-sectional anatomy of the cranioencephalic structures of the camel head using MR images and gross anatomic sections.

Materials and Methods

Magnetic resonance images of three normal camel brains and associated structures were selected. The camels were killed and the heads were sectioned at the level of atlantoaxial joint, cooled to −20°C and imaged within 24 h to minimize post-mortem changes.

Magnetic resonance imaging was performed at the Radiodiagnostic Service of the Clinica San Roque of Las Palmas de Gran Canaria using a superconducting magnet operating at a field strength of 1.5 T (Genesis Signa model, General Electric Medical System, Florence, SC, USA) and a human body coil was used to obtain the images. MR images were obtained in sagittal, transverse and oblique dorsal planes with spin-echo sequences. T1-weighted MR images were acquired using the following parameters: repetition time (T_R) = 500 ms, echo time (T_E) = 14 ms, 512 × 224 matrix, 1.0 cm slice thickness with 1 cm interslice spacing. For the T2-weighted MR images, the T_R was 3500 ms, T_E was 100 ms, 256 × 224 matrix, 7 mm slice thickness with 5 mm interslice spacing.

The MR images were compared with gross anatomical sections (Hillmann, 1975; Smuts and Bezuidenhout, 1987; Schaller, 1992; Vázquez Autón et al., 1992).

Results and Discussion

Clinically relevant anatomic structures of the head were identified and labelled. Figure 1 depicts the mid-sagittal MR image. Transverse MR images were oriented so that the right side of the head is to the viewer's left, and dorsal side at the top (Figs 2–4). Figure 5 is an oblique dorsal plane image.

In MR images, the grey scale is directly related to the signal intensity of the brain and associated structures of the camel head. MR T1-weighted images provided excellent anatomic depiction of the brain and associated formations. The cerebral structures (myelencephalon, pons, cerebellar vermis, cerebellar hemisphere, mesencephalon, cerebral hemisphere, thalamus, hypothalamus, pituitary gland, etc.) and different muscles of the head had an intermediate signal intensity and appeared grey. The cortical white matter was hypointense compared with grey matter. Cerebrospinal fluid (CSF) included the encephalic ventricular system and as the subarachnoid spaces had a negligible signal intensity they were obscured. The bones of the skull (occipital, parietal, temporal, frontal, basisphenoid, presphenoid), hyoid bones and mandible could be visualized indirectly because of fat in the bone marrow, as well as by observing the area of hypointense signal corresponding to the cortical margins of those bones. Fat, scalp and bone marrow had a hyperintense signal and were easily differentiated compared with the surrounding structures such as the pharynx, paranasal sinuses and cortical margins of the bones of the head.

In T2-weighted images, cerebral structures and muscles had a low signal intensity and were obscured. The cortical white

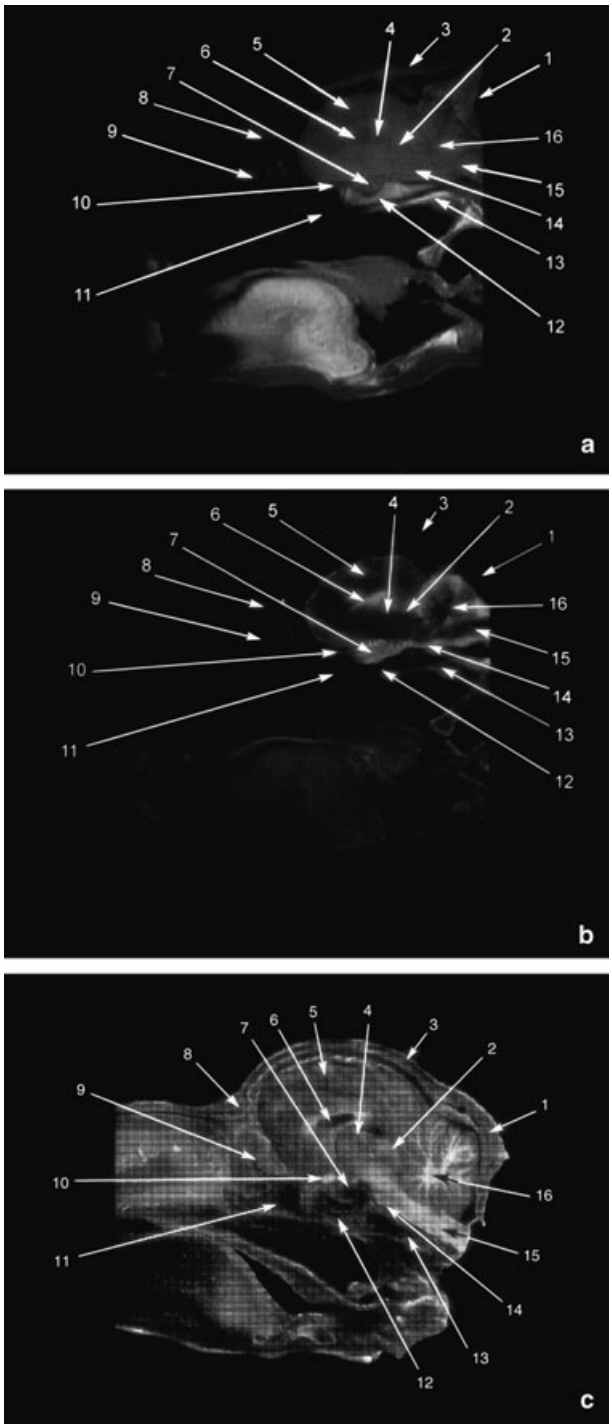

Fig. 1. (a) T1-weighted mid-sagittal MR image; (b) T2-weighted mid-sagittal MR image, and (c) gross section of the camel head. 1, Occipital squama; 2, mesencephalic tectum; 3, parietal bone; 4, thalamus; 5, cerebral hemisphere: cerebral cortex; 6, fourth ventricle; 7, pituitary gland; 8, frontal bone and frontal sinus; 9, ethmoid labyrinth; 10, optic chiasm; 11, body of presphenoid bone; 12, body of basisphenoid bone; 13, basilar part of occipital bone; 14, myelencephalon; 15, pons; 16, cerebellar vermis.

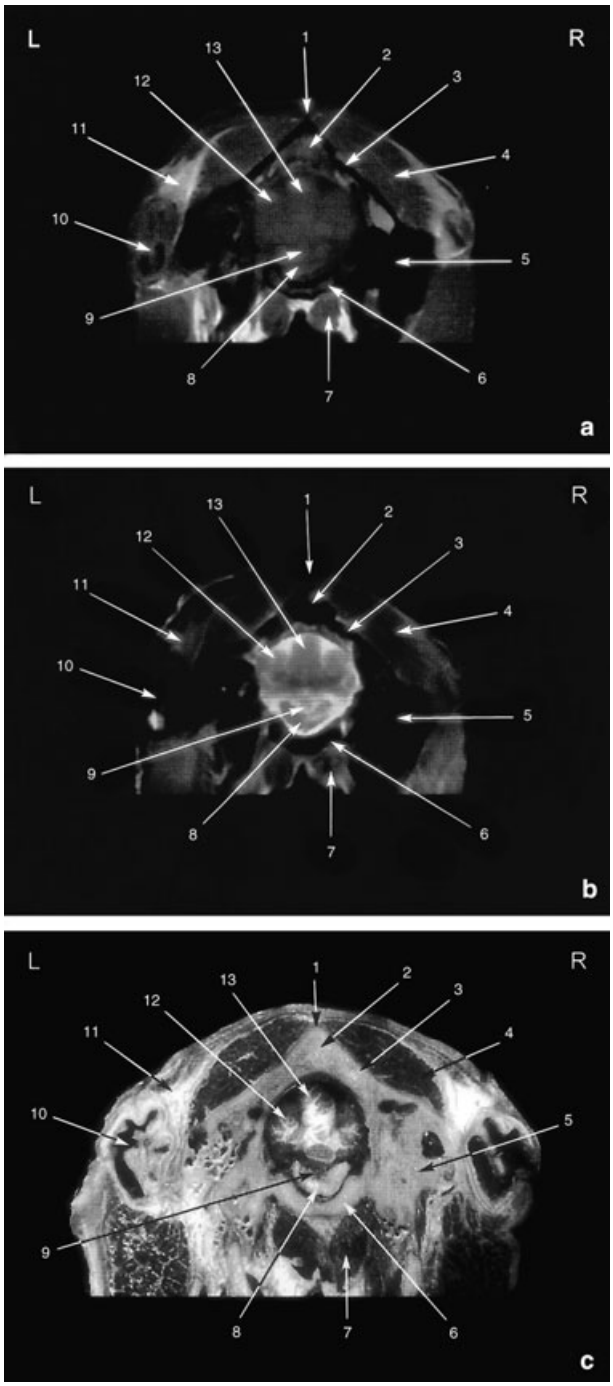

Fig. 2. (a) T1-weighted transverse MR image, (b) T2-weighted transverse MR image, and (c) gross section at the level of myelencephalon and fourth ventricle. 1, External sagittal crest; 2, occipital squama; 3, parietal bone; 4, temporal muscle; 5, petrous part of temporal bone; 6, basilar part of occipital bone; 7, rectus ventralis and longus capitis muscles; 8, myelencephalon; 9, fourth ventricle; 10, auricle; 11, auricular fat; 12, cerebellar hemisphere; 13, cerebellar vermis.

matter was hypointense compared with grey matter. CSF had a high signal intensity and appeared bright white in the subarachnoid spaces and the cerebral ventricles. The bones of the skull had high signal intensity in their medullary cavities and negligible signal in cortical bone. Fat reduced signal intensity compared with T1-weighted MR images.

Clinical diagnosis by imaging techniques is based on different physical principles that allow the visualization of the internal structure, the composition and even the function of a living being. MR is based on the properties of certain

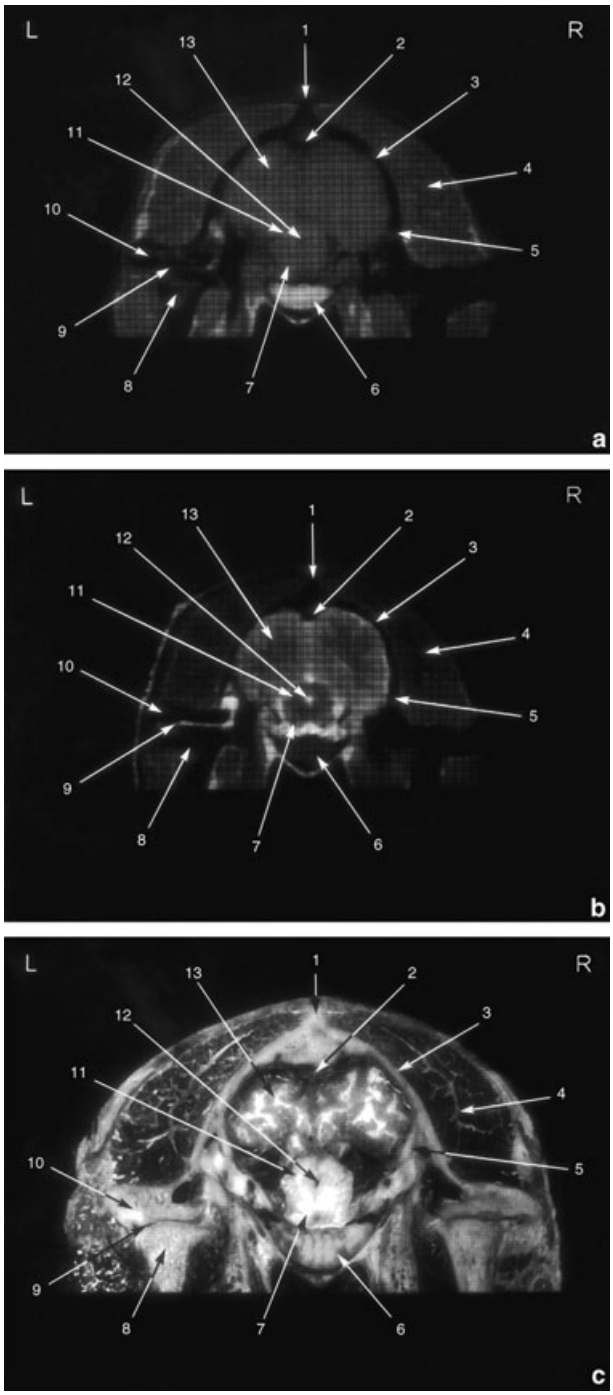

Fig. 3. (a) T1-weighted transverse MR image, (b) T2-weighted transverse MR image, and (c) gross sections at the level of mesencephalic aqueduct and temporomandibular joint. 1, External sagittal crest; 2, dorsal sagittal sinus; 3, parietal bone; 4, temporal muscle; 5, squamous part of temporal bone; 6, body of basisphenoid bone; 7, mesencephalic tegmentum; 8, condylar process of mandible; 9, temporomandibular joint: articular disc; 10, zygomatic process of temporal bone; 11, mesencephalic tectum: rostral collicules; 12, mesencephalon: mesencephalic aqueduct, 13, cerebral hemisphere: cerebral cortex.

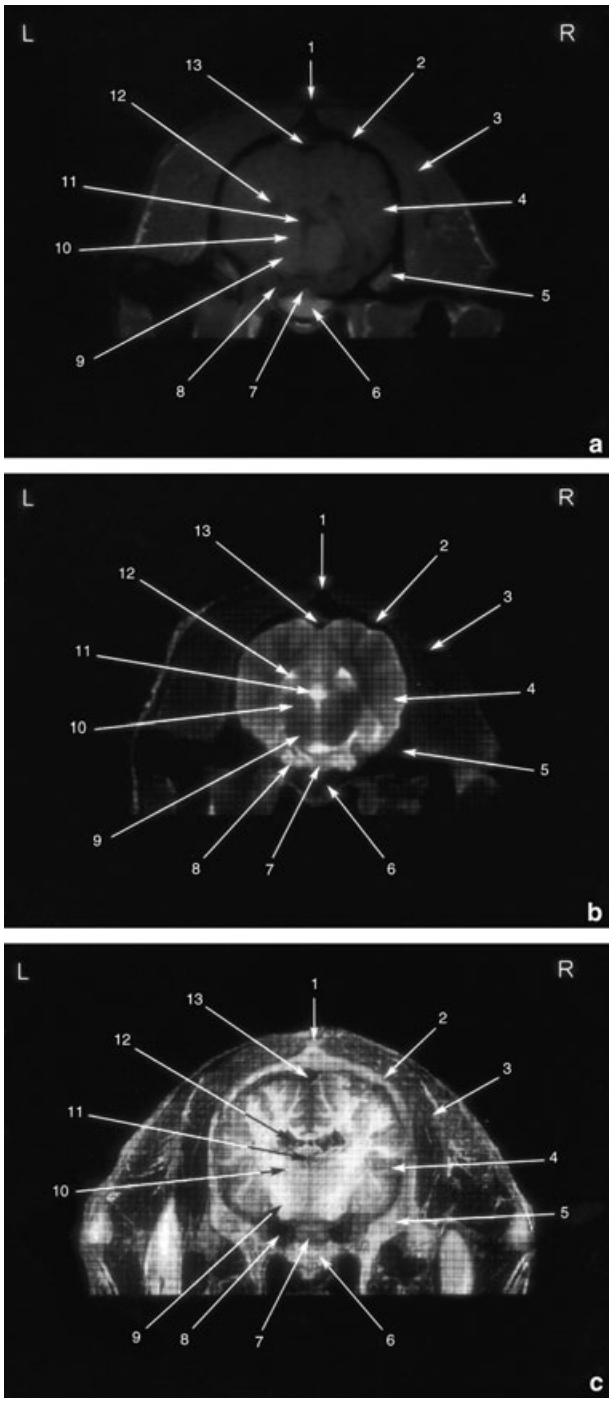

Fig. 4. (a) T1-weighted transverse MR image, (b) T2-weighted transverse MR image, and (c) gross sections at the level of thalamus and third ventricle. 1, External sagittal crest; 2, parietal bone; 3, temporal muscle; 4, cerebral hemisphere: cerebral cortex; 5, squamous part of temporal bone; 6, body of basisphenoid bone; 7, pituitary gland; 8, cavernous sinus and maxillary, trochlear, abducent and opthalmic nerves; 9, hypothalamus; 10, thalamus; 11, third ventricle; 12, lateral ventricle; 13, dorsal sagittal sinus.

elements, mainly hydrogen, to send a radiofrequency signal when it is under a magnetic field of certain intensity and stimulated by radiowaves an appropriate frequency (Thompson et al., 1993; Dennis, 1995). The advantages of MRI include multiplanar imaging, superior contrast resolution and the absence of ionizing radiation.

Magnetic resonance imaging provides substantially more gross anatomic detail of the camel head than other imaging techniques. Spin-echo T1-weighted MR images of the camel

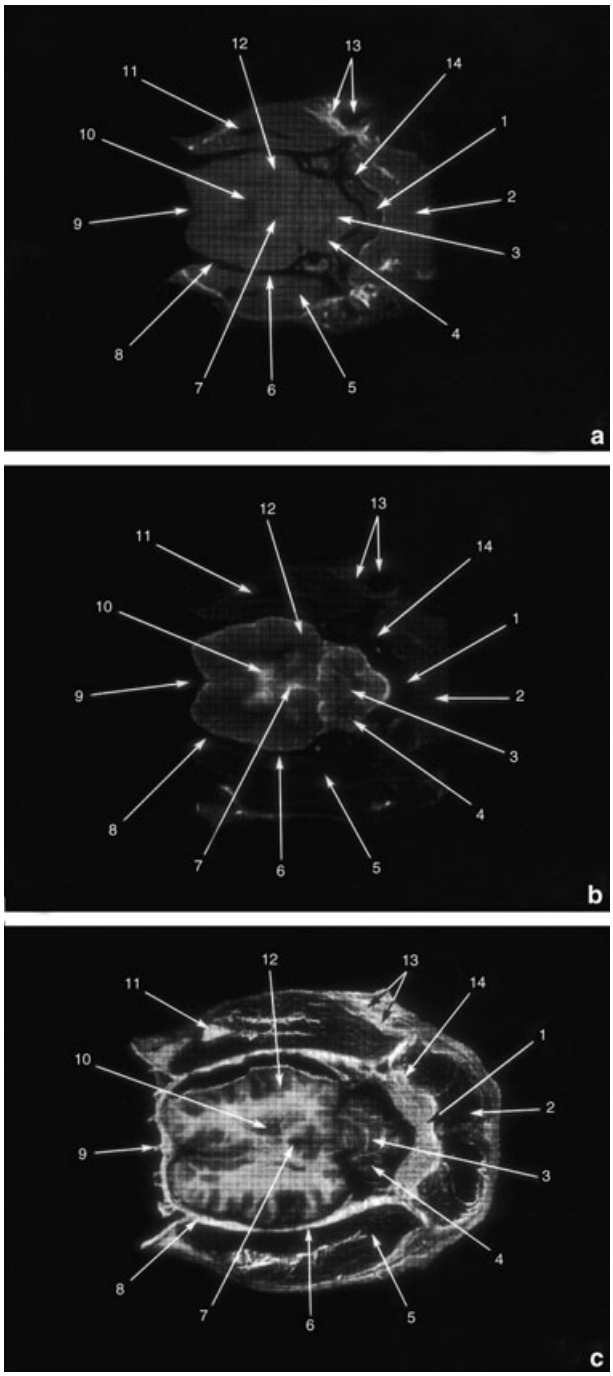

Fig. 5. (a) T1-weighted oblique dorsal MR image, (b) T2-weighted oblique dorsal MR image, and (c) gross section at the level of frontal squama. 1, Occipital squama; 2, neck dorsal muscles; 3, cerebellar vermis; 4, cerebellar hemisphere; 5, temporal muscle; 6, squamous part of temporal bone; 7, third ventricle; 8, parietal bone; 9, frontal squama and frontal sinus; 10, lateral ventricle; 11, coronoid process of ramus of mandible; 12, cerebral hemisphere: cerebral cortex; 13, auricle and auricular fat; 14, nuchal crest.

head provided excellent detail of clinically relevant anatomy. Excellent discrimination of both soft and mineralized tissues was evident in MR images. A thorough understanding of normal brain anatomy on MR images is essential to optimize the diagnosis of the diseases of the central nervous system. The anatomic relationships of the deep cerebral structures are recognized most easily in the transverse plane. The use of MRI in camel medicine is currently limited because of its expense, availability, and the logistic problems of acquiring MR images in large animals (Morgan et al., 1993; Widmer et al., 1999). Imaging live camels in MR is difficult because of the low availability of a suitable unit and a non-magnetic anaesthetic unit. With developing technology, including new developments in open magnet design, MR imaging may soon be more readily available for camel imaging. The information presented in this paper should serve as an initial reference to evaluate MR images of the camel head.

References

Arencibia, A., J. M. Vázquez, R. Jaber, J. A. Ramírez, M. Rivero, N. González and E. R. Wistner, 2000: Magnetic resonance imaging and cross sectional anatomy of the normal equine sinuses and nasal passages. Vet. Radiol. Ultrasound **41,** 313–319.

Arnold, D. L. and P. M. Matthews, 2002: MRI in the diagnosis and management of multiple sclerosis. Neurology **58,** 23–31.

Chaffin, M. K., M. A. Walker, N. H. MCarthur, E. E. Perris and N. S. Matthews, 1997: Magnetic resonance imaging of the brain of normal neonatal foals. Vet. Radiol. Ultrasound **38,** 102–111.

Dennis, R., 1995: Magnetic resonance imaging: an overview of its curent use in veterinary medicine. Vet. Int. **7,** 50–58.

Goncalves-Ferreira, A. J., M. Herculano-Carvalho, J. P. Melancia, J. P. Farias and L. Gomes, 2001: Corpus callosum: microsurgical anatomy and MRI. Surg. Radiol. Anat. **23,** 409–414.

Hillmann D. J., 1975: Skull. In: Sisson and Grosman's The Anatomy of the Domestic Animals, 5th edn (R. Getty, ed.). Philadelphia, PA: WB Saunders Co.

Hudson, L. C., L. Cauzinille, J. N. Kornegay and M. B. Tompkins, 1995: Magnetic resonance imaging of the normal feline brain. Vet. Radiol. Ultrasound **36,** 267–275.

Karkkainen, M., M. Mero, P. Nummi and L. Punto, 1991: Low field magnetic resonance imaging of the canine central nervous system. Vet. Radiol **32,** 71–74.

Kraft, S. L., P. Gavin, L. R. Wendling and V. K. Reddy, 1989: Canine brain anatomy on magnetic resonance images. Vet. Radiol. **30,** 147–158.

Morgan, R. V., G. B. Daniel and R. L. Donell, 1993: Magnetic resonance imaging of the normal eye and orbit of the horse. Prog. Vet. Comp. Ophthal. **3,** 127–133.

Morgan, R.V., G. B. Daniel and R. L. Donell, 1994: Magnetic resonance imaging of the normal eye and orbit of the dog and cat. Vet. Radiol. Ultrasound **35,** 102–108.

Schaller, O., 1992: Illustrated Veterinary Anatomical Nomenclature. Sttutgart: Ferdinand Enke.

Smuts, M. M. S. and A. J. Bezuidenhout, 1987: Anatomy of the Dromedary. Oxford: Clarendon Press.

Thompson, C. E., J. N. Kornegay, R. A. Burn, B. P. Drayer, D. M. Hadley, D. C. Levesque, L. A. Gainsburg, S. B. Lane, N. J. H. Sharp and S. J. Wheeler, 1993: Magnetic resonance imaging-a general overview of principles and examples in veterinary neurodiagnosis. Vet. Radiol. Ultrasound **34,** 2–17.

Vázquez Autón, J. M., F. Gil Cano, F. Moreno Medina, R. Latorre Reviriego and G. Ramírez Zarzosa, 1992: Atlas en Color. Anatomía Veterinaria, vol. 1. Cabeza, Murcia: Universidad de Murcia.

Widmer, W. R., K. A. Buckwalter, M. A. Hill, J. F. Fessler and S. Ivancevich, 1999: A technique for magnetic resonance imaging of equine cadaver specimens. Vet. Radiol. Ultrasound **40,** 10–14.